Exotic Band Structures and Exceptional Points for an Electric Lattice with Periodic Modulation in Time

Alexander Gómez Rojas[*] and Peter Halevi

Abstract—We study electromagnetic wave propagation in a system that is periodic both in space and in time, namely, a discrete ("lumped") transmission line with capacitors ("varactors") that are modulated in time harmonically. These periodicities result in exotic electromagnetic band structures that are periodic in the angular frequency ω and in the phase advance ka of the wave. Depending on the strength of modulation m and the reduced modulation frequency Ω/ω_0 (where ω_0 is the resonant frequency of a unit cell of the transmission line), this band structure can display frequency or wave vector band gaps, both, or neither. Moreover, minor changes in Ω or the modulation strength can control the aperture or closure of a gap and even transform a k-gap to an ω-gap. Such phase transitions are intimately associated with exceptional or critical points in the (ω, k, Ω, m) space.

1. INTRODUCTION

Electromagnetic wave propagation in periodic systems has a long history [1]. Photonic crystals with 1D, 2D, and 3D spatial periodicity have been extensively studied [2, 3]. These artificial compounds display photonic band structures and, with adequate dielectric contrast, complete frequency gaps. With appropriate engineering of the unit cell and long wavelengths in comparison to the cell size, a photonic crystal can even have an effective negative index of refraction. Electromagnetic wave propagation in such "metamaterials" has been widely investigated [4–7]. Parametric amplification [8] and negative refraction in a 2D transmission line [9] were reported in transmission lines. Among interesting applications, we also note reconfigurable filters [10], power dividers and transmission lines with negative group delay [11–13]. In contrast to the aforementioned publications — all concerning spatial periodicity — a relatively new line of research deals with propagation in media with at least one material parameter being periodic in time [11–13]. Such "temporal photonic crystals" have been assumed to be spatially uniform or to have the form of a slab; their band structures are characterized by wave-vector band gaps, and the transmitted light takes the form of a frequency comb [14–16]. If the frequency of the incident wave is equal to 1/2, or 3/2, etc. of the modulation frequency, the waves in the slab are stationary [17], and for special thicknesses of the slab, the optical response can be resonant [18, 19]. Exotic properties can also be found due to exceptional points in phase space at which two or more eigenmodes coalesce; this property could lead to ultra-sensitive sensors for the measurment of weak signals [20–24].

A different situation arises when the medium is modulated by a large-amplitude wave, the characteristic parameters becoming periodic in the phase of this pump wave (with period 2π). Such "space-time" media were first investigated in the 1960s [25–28] and, more recently, by Caloz's group [29–31]. They give rise to band gaps with oblique alignment. On the other hand, the spatial and temporal periodicities of the system can also be independent of each other, as in the case of discrete ("lumped") transmission lines with external, in-phase modulation of the capacitors ("varactors"). For propagation in a low-pass, modulated transmission line, the first observation of a "vertical" (wave vector) band-gap

* Corresponding author: Alexander Gómez Rojas (alexander2358@hotmail.com).
The authors are with the Department of Electronics, National Institute of Astrophysics, Optics and Electronics (INAOE), Luis Enrique Erro # 1, Tonantzintla, Puebla, C.P. 72840, México.

was recently reported [32, 33]. Further, a transmission line with modulated, nonlinear varactors can also support localized oscillations called "breathers" [34–37].

The aim of our present research is to explore the effects of the modulation frequency on the propagation of waves in an infinitely long, dynamic transmission line, pictured in Fig. 1. The capacitors in each unit cell are constituted by means of voltage-dependent varactors that are modulated *in tandem* harmonically. This is to say that our transmission line is periodic both in space and in time. What kind of electromagnetic wave propagation is possible in such a doubly periodic system?
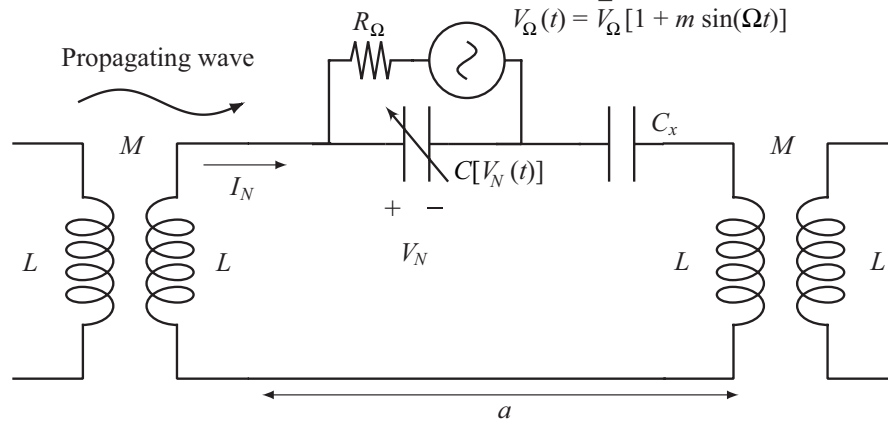

Figure 1. Nth unit cell of a dynamic transmission line with varactors whose voltage-dependent capacitances $C[V_N(t)]$ are modulated in tandem periodically by a harmonic source $V_\Omega(t)$.

2. TRANSMISSION LINE SYSTEM

Transmission line is formed by unit cells where each cell is composed by a capacitance C in the N'th unit cell which depends on the voltage V_N between its terminals; $C(V_N)$ itself depends on the modulating source voltage $V_\Omega(t)$. Each cell also incorporates two self-inductances L that are coupled to the neighboring cells by mutual inductances M. Moreover, we allow for an auxiliary capacitance C_x that eliminates DC currents and, hence, inhibits an average, DC component of V_N. A narrow band pass filter is used to eliminate current flow toward the modulation source. This band pass filter can be modeled as a non-reciprocal resistance R_Ω whose value is small when the voltage has frequency Ω and has a high value for other frequencies. Kirchhoff's voltage and current laws applied to this N'th cell give

$$V_N + 2L\frac{dI_N}{dt} + M\frac{dI_{N+1}}{dt} + M\frac{dI_{N-1}}{dt} + \frac{Q_{xN}}{C_x} = 0$$

$$I_N = I_{C_N} + \frac{V_N - V_\Omega}{R_\Omega} \tag{1}$$

Here, Q_{xN} is the charge on the auxiliary capacitor C_x; thus $dQ_{xN}/dt = I_N$. The current through the varactor is conveniently expressed in terms of the dynamic or differential capacitance $\tilde{C}(V_N)$ as

$$I_{C_N} = \frac{dQ_N}{dt} = \frac{d(CV_N)}{dt} \equiv \tilde{C}\frac{dV_N}{dt}, \quad \tilde{C} = C + V_N\frac{dC}{dV_N} \tag{2}$$

2.1. Transmission Line Analysis without Propagating Wave

First we study the transmission line in the absence of a propagating wave. With all the cells being identical, the voltages V_N and currents I_N are the same for all N, so that $V_N = V$ and $I_N = I$. Eliminating the current I reemplacing Eq. (1) lower equation into Eq. (1) higher equation, we are left with a complicated nonlinear differential equation for the varactor voltage $V(t)$; in this equation the nonlinear capacitance $\tilde{C}(V)$ is specified, corresponding to a hyper-abrupt varactor diode (SM1249).

In a subsequent paper we will compare in detail the solutions $V(t)$ of this differential equation with the modulation voltage $V_\Omega(t)$ for a choice of parameters. Here, we confine our attention to the most desirable situation — that these two voltages are nearly equal in magnitude and phase. In order to achieve this, the voltage drop over the resitance R_Ω should be made as small as possible in comparison to $V(t)$. If the modulation frequency Ω is near the resonance frequency $\omega_0(= 1/\sqrt{2C_0[L + M]})$ of the lower current loop in Fig. 1, then, indeed, most of the current will be drained from the resistor; here the auxiliary capacitor has been neglected on account of its very small impedance in comparison to the average impedance of the varactor ($C_x \gg \overline{\tilde{C}}(V) \equiv \tilde{C}_0$). This qualitative argument is vindicated by exact solutions of the differential equation for $V(t)$ for a series of reduced modulation frequencies $\hat{\Omega} = \Omega/\omega_0$. In Fig. 2, we compare the maximal values of $V(t)$ and $V_\Omega(t) = \bar{V}_\Omega[1 + m\sin(\Omega t)]$, where $\bar{V}_\Omega$ is the average modulation voltage, and m is the modulation strength. The coincidences in magnitude and phase are excellent over two orders of magnitude, $0.1 < \Omega/\omega_0 < 10$. The inset shows the varactor voltage (dots) and modulation voltage (line) as a function of time. The practically perfect fit has been aided by a choice of a very small value for the resistance R_Ω when the frequency is Ω. We can then safely write $V(t) = V_\Omega(t)$ as long as there is no propagating wave.
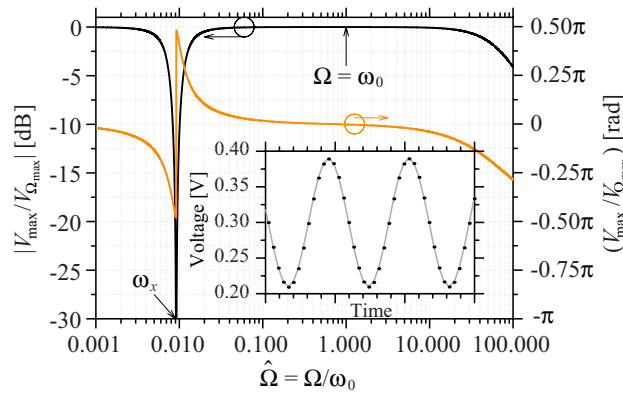

Figure 2. Comparison of the voltage over a varactor with the voltage V_Ω of the modulation source as function of the normalized modulation frequency $\hat{\Omega} = \Omega/\omega_0 = \Omega\sqrt{2C_0[L + M]}$. The two voltages are practically the same in the range $0.1 < \hat{\Omega} < 10$. Inset: $V_\Omega(t)$ (line) and $V(t)$ (dots) for $\hat{\Omega} = 1$. Parameters used: $L = 10\,\text{nH}$, $M = 6\,\text{nH}$, $C_x = 10\,\text{nF}$, $R_\Omega = 1\,\text{Ohms}$, $\bar{V}_\Omega = 0.3\,\text{V}$, $m = 0.3$, $C_0 = 2\,\text{pF}$ (varactor diode SM1249).

2.2. Transmission Line Analysis with Propagating Wave

In the presence of a propagating wave of voltage $v_N(t)$, the varactor voltage becomes modulated in space, as well as in time. Its value in the N'th cell is

$$V_N(t) = V_\Omega(t) + v_N(t) = \bar{V}_\Omega[1 + m\sin(\Omega t)] + v(t)e^{ikaN} \tag{3}$$

where ka is the phase advance over a single unit cell. Assuming a wave of small amplitude, $|v(t)| \ll \bar{V}_\Omega$, the capacitance $\tilde{C}(V)$ changes little and can be approximated as

$$\tilde{C}(V_N) = \tilde{C} + \frac{d\tilde{C}}{dV}v_N \tag{4}$$

Substituting Eqs. (3) and (4) in Eq. (1), we find that the amplitude $v(t)$ of the small signal $v_N(t)$ satisfies the equation

$$P(t)\frac{d^3v}{dt^3} + S(t)\frac{d^2v}{dt^2} + T(t)\frac{dv}{dt} + U(t)v = 0 \tag{5}$$

where we have neglected terms of the order of v^2 and higher. The functions $P(t)$, $S(t)$, $T(t)$, and $U(t)$

are defined in ref.[†]; they depend on time only through $\tilde{C}(V_\Omega(t))$ and are therefore periodic, with the period $2\pi/\Omega$. The solution must then be given by the Bloch-Floquet theorem in time,

$$v = \tilde{v}(t)e^{-i\omega t} = \sum_r \tilde{v}_r(\omega)e^{-i(\omega - r\Omega)t} \tag{6}$$

According to this theorem, the function $\tilde{v}(t)$ must also have the period $2\pi/\Omega$, thus allowing the Fourier expansion given by the second equality. The frequency ω plays a similar role to the Bloch wave vector k in the case of spatial periodicity and is the wave frequency in practice. Substituting Eq. (6) in Eq. (5) and also expanding the functions P, S, T, and U in Fourier series, we obtain an eigenvalue equation for the Fourier coefficients $\tilde{v}_r(\omega)$:

$$\sum_r \left[-i(r\Omega - \omega)^3 P_{s-r} - (r\Omega - \omega)^2 S_{s-r} + i(r\Omega - \omega)T_{s-r} + U_{s-r} \right] \tilde{v}_r(\omega) = 0 \tag{7}$$

Here, P_n, S_n, T_n, and U_n are, respectively, the Fourier coefficients of $P(t)$, $S(t)$, $T(t)$, and $U(t)$. The indices r and s run over all integer values; thus we have an infinite number of equations in s for the infinite number of unknowns $\tilde{v}_r(\omega)$. Then the determinant of the expression in the square brackets must vanish, leading to a functional relation between ω and ka, that is, the dispersion relation for the propagating wave. The structure of Eq. (7) implies that $k(\omega + \Omega) = k(\omega)$, that is, periodicity in ω with the period Ω. Further, it follows from the coefficients P_n, S_n, T_n, and U_n that $\omega(ka + 2\pi) = \omega(ka)$, meaning periodicity in ka with the period 2π. Our dispersion relation $\omega(ka)$ then has the form of a "double band structure"; the periodicities in both time and space transform into periodicities in both the frequency and wave vector. There is also mirror symmetry around the frequencies $\omega = \pm\Omega/2, \pm3\Omega/2$, etc.

Before turning to the numerical solution of Eq. (7), it is instructive to analyze the limit of vanishing modulation strength, $m \to 0$. (Its spatial analogue is called the "empty lattice approximation"). In this limit $\tilde{C}(V_\Omega(t)) \to \tilde{C}(\bar{V}_\Omega) = \tilde{C}_0$ and $P_{s-r} = P_0\delta_{sr}$, etc. for S, T and U in Eq. (7). This equation then is reduced to

$$-iP_0(r\Omega - \omega)^3 - S_0(r\Omega - \omega)^2 + iT_0(r\Omega - \omega) + U_0 = 0 \tag{8}$$

with P_0, S_0, T_0, and U_0 given in ref.[‡]. With frequency ω of the propagating wave being real, this equation has complex solutions for k, its imaginary part describing damping. However, the resistance R_Ω in Fig. 1 models a non-reciprocal element that prevents currents flowing toward the modulation sources. Hence, for frequencies different from Ω we can assume a large resistance ($R_\Omega = 1\,\mathrm{kOhm}$) experienced by the propagating voltage which has frequency ω, while the modulation voltage with frequency Ω in Fig. 1 is subject to a small resistance ($R_\Omega = 1\,\mathrm{Ohm}$). It is then a a good approximation to take $S_0 = U_0 = 0$, thus neglecting damping. Eq. (8) is thus reduced to

$$\hat{\omega} = r \pm \frac{1}{\hat{\Omega}}\sqrt{\frac{1 + \hat{M}}{1 + \hat{M}\cos(ka)}} \tag{9}$$

for the normalized frequency $\hat{\omega} = \omega/\Omega$, with $\hat{M} = M/L$. For $r = 0$, the positive sign gives the dispersion relation for the unmodulated (static) band-pass transmission line. It has the lower band edge $\hat{\omega} = 1/\hat{\Omega}$ or $\omega = \omega_0$ for $ka = 0$ and the upper edge $\hat{\omega} = (1/\hat{\Omega})\sqrt{(1 + \hat{M})/(1 - \hat{M})}$ or $\omega = \omega_0\sqrt{(1 + \hat{M})/(1 - \hat{M})}$ for $ka = \pm\pi$. Figs. 3(a)–(l) compare the modulations $m = 0$ and $m = 0.4$, and Figs. 3(m)–(x) compare $m = 0.4$ and 0.6 in a single period of $\hat{\omega}$ (corresponding to $0 < \omega < \Omega$) that has to be repeated in the vertical direction, with no change of form, for all the integers r. There are two periods of ka ($-2\pi < ka < 2\pi$), to be extended infinitely in the horizontal direction to obtain the complete double band structure. The black lines in the atlas of Figs. 3(a)–(l) correspond to Eq. (9) for $r = 0$ with the positive root for a sequence of the parameter $\hat{\Omega}$ ranging from 5.5 in (a) to 0.5 in (l). Also in black lines, we plot Eq. (9) for $r = 1$ with the negative root; these are mirror images of the former curves

---

[†] $K(ka) = 2L + 2M\cos(ka)$, $P(t) = K(ka)\tilde{C}$, $S(t) = 3dP(t)/dt + K(ka)/R_\Omega$, $T(t) = 3d^2P(t)/dt^2 + \tilde{C}/C_x + 1$, $U(t) = d^3P(t)/dt^3 + (1/C_x)d\tilde{C}/dt + 1/(R_\Omega C_x)$, $F(t) = P(t)d^3V_\Omega(t)/dt^3 + (2dP(t)/dt)d^2V_\Omega(t)/dt + (d^2P(t)/dt^2 + 1 + \tilde{C}/C_x)dV_\Omega(t)$.

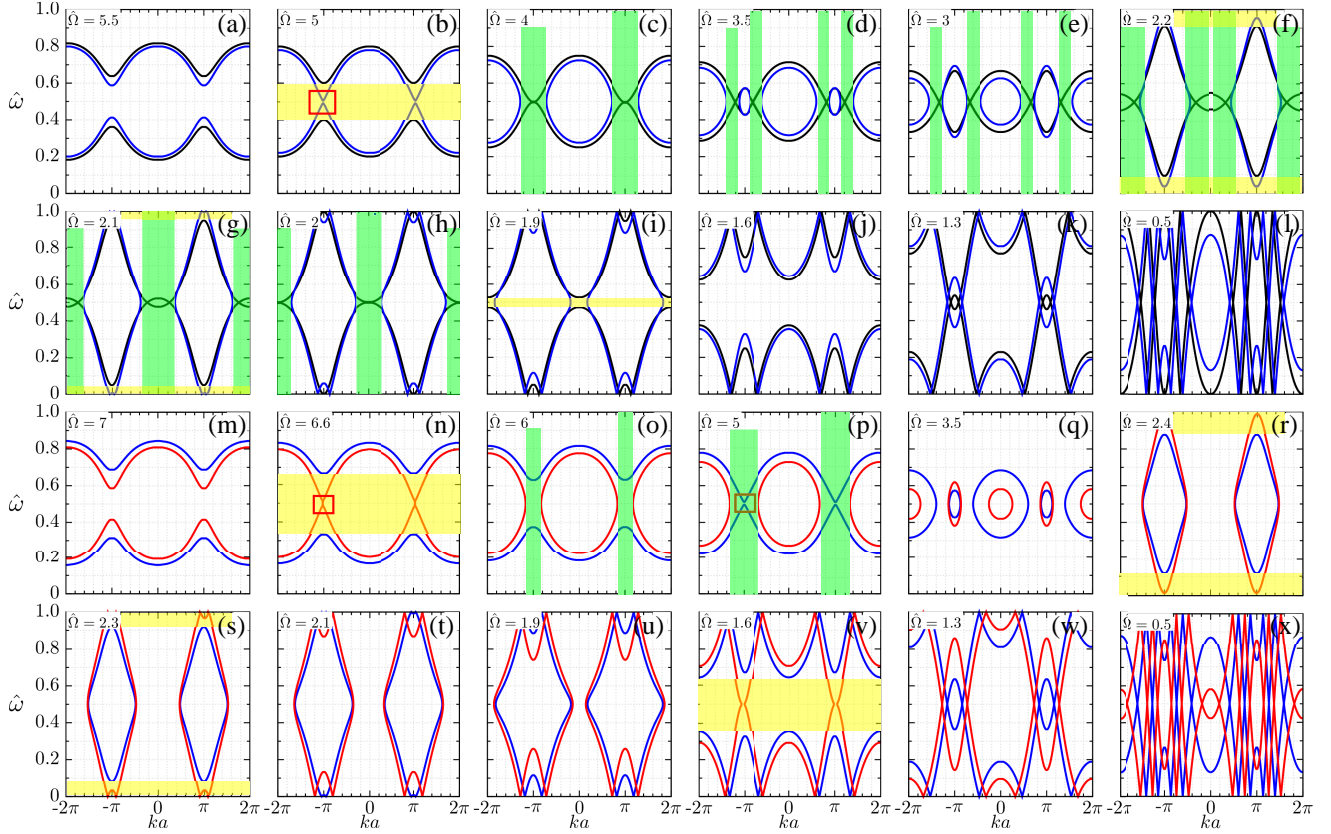[‡] $P_0 = K(ka)\tilde{C}_0$, $S_0 = K(ka)/R_\Omega$, $T_0 = \tilde{C}_0/C_x + 1$, $U_0 = 1/(R_\Omega C_x)$.

Figure 3. In (a)–(l) electromagnetic band structures $\hat{\omega}(ka)$ are compared for the modulation strengths $m = 0$ ("empty temporal lattice") and $m = 0.4$ ("weak modulation") for 12 values of the reduced modulation frequency $\hat{\Omega} = \Omega/\omega_0$. In (m)–(x) a similar comparison is shown for $m = 0.4$ and $m = 0.6$ ("strong modulation") for 12 in general different values of $\hat{\Omega}$. The horizontal yellow bands indicate frequency band-gaps created by a change in m. Similarly, the vertical green bands denote wave-vector band-gaps produced by a change in m. We used the approximation $V(t) = V_\Omega(t)$, as justified by Fig. 2. Parameters as in Fig. 2, with $R_\Omega = 1\,\text{kOhm}$.

with respect to the frequency $\hat{\omega} = 1/2$ and are absent for the static transmission line. For this empty *temporal* lattice, the frequency values at the center and edges of the Brillouin zone are

$$\hat{\omega}_{(ka=0)} = r \pm \frac{1}{\hat{\Omega}}, \quad \hat{\omega}_{(ka=\pm\pi)} = r \pm \frac{1}{\hat{\Omega}}\sqrt{\frac{1 + \hat{M}}{1 - \hat{M}}} \tag{10}$$

3. RESULTS

For $\hat{\Omega} = 5.5$ and $m = 0$ in Fig. 3(a), there is a frequency gap between the "twin bands" pictured. As $\hat{\Omega}$ is decreased, this gap is reduced, until it vanishes for $\hat{\Omega} = 4$, see (c); the two bands touch at $ka = \pm\pi$. With further decrease of $\hat{\Omega}$, these bands overlap more and more, reaching the limits $\hat{\omega} = 0$ and $\hat{\omega} = 1$ at $\hat{\Omega} = 2$, (h). At that point propagation is allowed for any frequency in the empty lattice limit. For $\hat{\Omega} < 2.1$ the peaks of the twin bands exit the frequency region shown (the first *temporal* Brillouin zone), only to re-emerge from the neighboring Brillouin zones at the opposite ends of the first zone. This creates a new stop band, centered at $\hat{\omega} = 0.5$, as in (i) and (j). However, for $\hat{\Omega} \approx 1.33$ the upper and lower bands again touch at $ka = \pm\pi$, thus eliminating the stop propagation band. Further reduction of $\hat{\Omega}$ will not result in passbands, of either ω or k, see (k). More and more k-bands are created, becoming narrower and narrower (l).

For finite modulations, the eigenvalue equation (7) has been solved for $m = 0.4$ and $m = 0.6$. The corresponding band structures are graphed, respectably, in blue and red lines in the Fig. 3 atlas. Generally speaking, the band structures $\hat{\omega}(ka)$ for $m = 0.4$ are quite similar to the limit $m \to 0$. However, a qualitatively new feature emerges, namely, now prohibited wave vector bands are produced. We also note that the group velocity $d\omega/dk$ vanishes at the borders of the spatial Brillouin zones ($ka = 0, \pm\pi, \pm 2\pi$) but is infinite at the border of the temporal Brillouin zone ($\omega/\Omega = 1/2$). The latter is explained by the mirror symmetry with respect to $\omega = \Omega/2$ or by the interchange of roles played by ω/Ω and ka. It is important to note that a change in $\hat{\Omega}$ or in m can generate forbidden frequency or wave-vector bands. For example, the comparison of (b) and (c) shows that for $m \leq 0.4$ an increase of $\hat{\Omega}$ from 4 to 5 brings about a transition from a k-gap to an ω-gap. On the other hand, the yellow and green bands indicate, respectively, the opening up of ω- and k-gaps due to a change of m, with $\hat{\Omega}$ held constant. The band structure behavior for $m = 0.6$ is quite similar to $m = 0.4$, but the transitions from ω-gap to k-gap occur in higher values of $\hat{\Omega}$ in comparison with $m = 0.4$, see Figs. 3(m)–(x). Interestingly, the changes occasioned by increasing m from 0.4 to 0.6 often resemble those incurred by an increase from $m = 0$ to $m = 0.4$: Compare (m), (n), (q), and (w) with, respectively, (a), (b), (e), and (k).

The delicate nature of the ω- and k-gaps is illustrated in Fig. 4(a) by zooming in on the behavior of the dispersion curves in the region of the small square in Fig. 3(b) and small variations of parameter $\hat{\Omega}$ for the weak modulation $m = 0.4$. There is a k-gap for $\hat{\Omega} = 4.9918129$ (#5). This gap is closed for $\hat{\Omega} = \hat{\Omega}_{crit} = 4.9968097$ (#6). However, further increase of $\hat{\Omega}$, to the value $\hat{\Omega} = 4.9973649$ (#7), does not lead to an overlap of the two bands, but to the creation of an ω-gap! The intersection of the lines # 6 defines a critical or exceptional point, for which no band gaps (either of ω or of k) exist. In the 3D representation of Fig. 4(b), this is also a saddle point. Such a point is given by specific values of the variables ω and k and parameters $\hat{\Omega}$ and m in (ω, k, Ω, m) space.
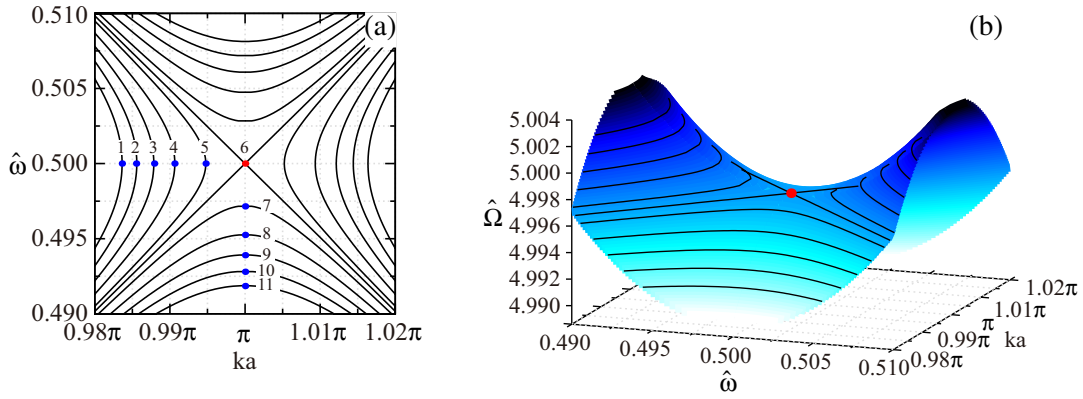

Figure 4. Zoom in on dispersion curves at $\hat{\omega} = 1/2$ and $ka = \pi$ for $m = 0.4$; see small rectangles in Figs. 3(b) and (n). The reduced modulation frequency goes from $\hat{\Omega} = 4.9918129$ (#1) to $\hat{\Omega} = 5.0018065$ (#11) through $\hat{\Omega} = \hat{\Omega}_{crit} = 4.9968097$ (#6). Proceeding from $\hat{\Omega} < \hat{\Omega}_{crit}$ to $\hat{\Omega} > \hat{\Omega}_{crit}$ there is a phase transition from k-gaps to ω-gaps. The 3D representation in (b) demonstrates that the exceptional point for $\hat{\Omega} = \hat{\Omega}_{crit}$ is also a saddle point.

4. CONCLUSION

The discrete transmission line in Fig. 1, with capacitors that are periodically modulated in time, is convenient for the investigation of wave propagation in systems with periodicity both in space and in time. In Fig. 2 we found that, with suitable choice of parameters, the voltage on the varactors can be made practically equal to the modulation voltage over three orders of magnitude of the reduced frequency $\hat{\Omega}$. The band structure for electromagnetic waves that can propagate along such a modulated transmission line depends qualitatively on $\hat{\Omega}$, as well on the modulation strength m. This results in the exotic electromagnetic band structures in Fig. 3, displaying gaps in the frequency or phase advance, simultaneous gaps in both, or no gap at all. Very small changes in either $\hat{\Omega}$ or m can control the

aperture or closure of an ω- or k-gap, and even transition from a k-gap to an ω-gap, as seen in Fig. 4. This behavior generates a critical or exceptional point at which no gap at all exists. This variability could lead to easily reconfigurable applications for filters, frequency multipliers, delay transmission lines, and metamaterial properties. Analogously, propagation of other kinds of waves in other kinds of systems that are periodic in both space and time could give rise to interesting band structures and useful applications.

ACKNOWLEDGMENT

REFERENCES

1. Brillouin, L., *Wave Propagation in Periodic Structures: Electric Filters and Crystal Lattices*, 255, Dover Publications, 1953.

2. Joannopoulos, J. D., S. G. Johnson, J. N. Winn, and R. D. Meady, *Photonic Crystals*, 2nd Edition, Princeton University Press, 2008.

3. Solymar, L. and E. Shamonina, *Waves in Metamaterials*, Oxford University Press, 2009.

4. Lai, A., T. Itoh, and C. Caloz, "Composite right/left-handed transmission line metamaterials," *IEEE Microwave Magazine*, Vol. 5, No. 3, 34–50, September 2004.

5. Kozyrev, A. B., H. Kim, A. Karbassi, and D. W. van der Weide, "Wave propagation in nonlinear left-handed transmission line media," *Applied Physics Letters*, Vol. 87, No. 12, 121109, September 2005.

6. Syms, R. R. A., E. Shamonina, V. Kalinin, and L. Solymar, "A theory of metamaterials based on periodically loaded transmission lines: Interaction between magnetoinductive and electromagnetic waves," *Journal of Applied Physics*, Vol. 97, No. 6, (064909)1–6, March 2005.

7. Gil, I., J. Bonache, M. Gil, J. García-García, F. Martín, and R. Marqués, "Accurate circuit analysis of resonant-type left handed transmission lines with inter-resonator coupling," *Journal of Applied Physics*, Vol. 100, No. 7, 074908, October 2006.

8. Kozyrev, A. B., H. Kim, and D. W. van der Weide, "Parametric amplification in left-handed transmission line media," *Applied Physics Letters*, Vol. 88, No. 26, 264101, June 2006.

9. Algredo-Badillo, U. and P. Halevi, "Negative refraction and focusing in magnetically coupled L-C loaded transmission lines," *Journal of Applied Physics*, Vol. 102, No. 8, 086104, October 2007.

10. Ou, Y. and G. M. Rebeiz, "Lumped-element fully tunable bandstop filters for cognitive radio applications," *IEEE Transactions on Microwave Theory and Techniques*, Vol. 59, No. 10, 2461–2468, October 2011.

11. Chaudhary, G., Y. Jeong, and J. Lim, "Microstrip line negative group delay filters for microwave circuits," *IEEE Transactions on Microwave Theory and Techniques*, Vol. 62, No. 2, 234–243, February 2014.

12. Chaudhary, G. and Y. Jeong, "Distributed transmission line negative group delay circuit with improved signal attenuation," *IEEE Microwave and Wireless Components Letters*, Vol. 24, No. 1, 20–22, January 2014.

13. Chaudhary, G. and Y. Jeong, "A design of power divider with negative group delay characteristics," *IEEE Microwave and Wireless Components Letters*, Vol. 25, No. 6, 394–396, June 2015.

14. Zurita-Sánchez, J. R., P. Halevi, and J. C. Cervantes-González, "Reflection and transmission of a wave incident on a slab with a time-periodic dielectric function $\epsilon(t)$," *Physical Review A*, Vol. 79, 053821, May 2009.

15. Martínez-Romero, J. S., O. M. Becerra-Fuentes, and P. Halevi, "Temporal photonic crystals with modulations of both permittivity and permeability," *Physical Review A*, Vol. 93, 063813, June 2016.

16. Koutserimpas, T. T. and R. Fleury, "Electromagnetic waves in a time periodic medium with step-varying refractive index," *IEEE Transactions on Antennas and Propagation*, Vol. 66, No. 10, 5300–5307, October 2018.

17. Martínez-Romero, J. S. and P. Halevi, "Standing waves with infinite group velocity in a temporally periodic medium," *Physical Review A*, Vol. 96, 063831, December 2017.

18. Zurita-Sánchez, J. R. and P. Halevi, "Resonances in the optical response of a slab with time-periodic dielectric function $\epsilon(t)$," *Physical Review A*, Vol. 81, 053834, May 2010.

19. Martínez-Romero, J. S. and P. Halevi, "Parametric resonances in a temporal photonic crystal slab," *Physical Review A*, Vol. 98, 053852, November 2018.

20. Miller, J. L., "Exceptional points make for exceptional sensors," *Physics Today*, Vol. 70, No. 10, 23, October 2017.

21. Hodaei, H., A. U. Hassan, S. Wittek, H. Garcia-Gracia, R. El-Ganainy, D. N. Christodoulides, and M. Khajavikhan, "Enhanced sensitivity at higher-order exceptional points," *Nature*, Vol. 548, 187–191, November 2017.

22. Chen, W., S. K. Özdemir, G. Zhao, J. Wiersig, and L. Yang, "Exceptional points enhance sensing in an optical microcavity," *Nature*, Vol. 548, 192–196, August 2017.

23. Kazemi, H., M. Y. Nada, F. Capolino, and F. Maddaleno, "Experimental demonstration of exceptional points of degeneracy in linear time periodic systems and exceptional sensitivity," *Arxiv.org.*, Vol. 1908, 08516, September 2020.

24. Miri, M. A. and A. Alù, "Exceptional points in optics and photonics," *Science*, Vol. 363, No. 6422, January 2019.

25. Morgenthaler, F. R., "Velocity modulation of electromagnetic waves," *IRE Transactions on Microwave Theory and Techniques*, Vol. 6, No. 2, 167–172, April 1958.

26. Currie, M. R. and R. W. Gould, "Coupled-cavity traveling-wave parametric amplifiers: Part I. Analysis," *Proceedings of the IRE*, Vol. 48, No. 12, 1960–1973, December 1960.

27. Cassedy, E. S. and A. A. Oliner, "Dispersion relations in time-space periodic media: Part I — Stable interactions," *Proceedings of the IEEE*, Vol. 51, No. 10, 1342–1359, October 1963.

28. Holberg, D. and K. Kunz, "Parametric properties of fields in a slab of time-varying permittivity," *IEEE Transactions on Antennas and Propagation*, Vol. 14, No. 2, 183–194, March 1966.

29. Chamanara, N., S. Taravati, Z.-L. Deck-Léger, and C. Caloz, "Optical isolation based on space-time engineered asymmetric photonic band gaps," *Physics Review B*, Vol. 96, 155409, October 2017.

30. Taravati, S., N. Chamanara, and C. Caloz, "Nonreciprocal electromagnetic scattering from a periodically space-time modulated slab and application to a quasisonic isolator," *Physics Review B*, Vol. 96, 165144, October 2017.

31. Chamanara, N., Z.-L. Deck-Léger, C. Caloz, and D. Kalluri, "Unusual electromagnetic modes in space-time-modulated dispersion-engineered media," *Physical Review A*, Vol. 97, 063829, June 2018.

32. Reyes-Ayona, J. R. and P. Halevi, "Observation of genuine wave vector (k or β) gap in a dynamic transmission line and temporal photonic crystals," *Applied Physics Letters*, Vol. 107, 074101, August 2015.

33. Reyes-Ayona, J. R. and P. Halevi, "Electromagnetic wave propagation in an externally modulated low-pass transmission line," *IEEE Transactions on Microwave Theory and Techniques*, Vol. 64, No. 11, 3449–3459, November 2016.

34. Stearrett, R. and L. Q. English, "Experimental generation of intrinsic localized modes in a discrete electrical transmission line," *Journal of Physics D: Applied Physics*, Vol. 40, No. 17, 5394–5398, August 2007.

35. Sato, M., S. Yasui, M. Kimura, T. Hikihara, and A. J. Sievers, "Management of localized energy in discrete nonlinear transmission lines," *EPL (Europhysics Letters)*, Vol. 80, No. 3, 30002, October 2007.

36. English, L. Q., F. Palmero, P. Candiani, J. Cuevas, R. Carretero-González, P. G. Kevrekidis, and A. J. Sievers, "Generation of localized modes in an electrical lattice using subharmonic driving," *Physical Review Letters*, Vol. 108, 084101, February 2012.

37. Gómez-Rojas, A. and P. Halevi, "Discrete breathers in an electric lattice with an impurity: Birth, interaction, and death," *Physical Review E*, Vol. 97, 022225, February 2018.